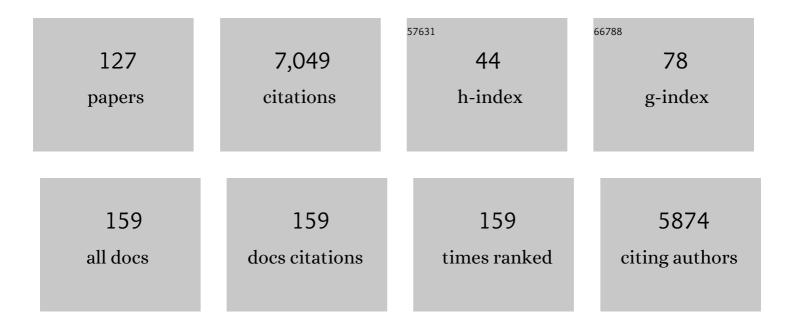
List of Publications by Year in descending order

Source: https://exaly.com/author-pdf/1321839/publications.pdf Version: 2024-02-01



#	Article	IF	CITATIONS
1	Daily canopy photosynthesis model through temporal and spatial scaling for remote sensing applications. Ecological Modelling, 1999, 124, 99-119.	1.2	626
2	A process-based boreal ecosystem productivity simulator using remote sensing inputs. Remote Sensing of Environment, 1997, 62, 158-175.	4.6	466
3	Effects of foliage clumping on the estimation of global terrestrial gross primary productivity. Global Biogeochemical Cycles, 2012, 26, .	1.9	273
4	Multi-angular optical remote sensing for assessing vegetation structure and carbon absorption. Remote Sensing of Environment, 2003, 84, 516-525.	4.6	244
5	Tropospheric Ozone Assessment Report: Present-day distribution and trends of tropospheric ozone relevant to climate and global atmospheric chemistry model evaluation. Elementa, 2018, 6, .	1.1	240
6	Net primary productivity of China's terrestrial ecosystems from a process model driven by remote sensing. Journal of Environmental Management, 2007, 85, 563-573.	3.8	234
7	Modelling multi-year coupled carbon and water fluxes in a boreal aspen forest. Agricultural and Forest Meteorology, 2006, 140, 136-151.	1.9	213
8	Net primary productivity distribution in the BOREAS region from a process model using satellite and surface data. Journal of Geophysical Research, 1999, 104, 27735-27754.	3.3	176
9	Evolution of evapotranspiration models using thermal and shortwave remote sensing data. Remote Sensing of Environment, 2020, 237, 111594.	4.6	156
10	Annual carbon balance of Canada's forests during 1895-1996. Global Biogeochemical Cycles, 2000, 14, 839-849.	1.9	150
11	Net primary productivity mapped for Canada at 1-km resolution. Global Ecology and Biogeography, 2002, 11, 115-129.	2.7	140
12	Local and synoptic meteorological influences on daily variability in summertime surface ozone in eastern China. Atmospheric Chemistry and Physics, 2020, 20, 203-222.	1.9	139
13	Spatial distribution of carbon sources and sinks in Canada's forests. Tellus, Series B: Chemical and Physical Meteorology, 2003, 55, 622-641.	0.8	133
14	Mapping evapotranspiration based on remote sensing: An application to Canada's landmass. Water Resources Research, 2003, 39, .	1.7	114
15	Tropospheric Ozone Assessment Report: Tropospheric ozone from 1877 to 2016, observed levels, trends and uncertainties. Elementa, 2019, 7, .	1.1	103
16	Net primary productivity following forest fire for Canadian ecoregions. Canadian Journal of Forest Research, 2000, 30, 939-947.	0.8	89
17	Angular normalization of GOMEâ€2 Sunâ€induced chlorophyll fluorescence observation as a better proxy of vegetation productivity. Geophysical Research Letters, 2017, 44, 5691-5699.	1.5	89
18	Tropospheric ozone in CMIP6 simulations. Atmospheric Chemistry and Physics, 2021, 21, 4187-4218.	1.9	89

#	Article	IF	CITATIONS
19	Evidence of vertical transport of carbon monoxide from Measurements of Pollution in the Troposphere (MOPITT). Geophysical Research Letters, 2004, 31, .	1.5	87
20	Importance of meteorology in air pollution events during the city lockdown for COVID-19 in Hubei Province, Central China. Science of the Total Environment, 2021, 754, 142227.	3.9	82
21	Approaches for reducing uncertainties in regional forest carbon balance. Global Biogeochemical Cycles, 2000, 14, 827-838.	1.9	80
22	Optical properties and radiative forcing of urban aerosols in Nanjing, China. Atmospheric Environment, 2014, 83, 43-52.	1.9	75
23	Analysis of the summertime buildup of tropospheric ozone abundances over the Middle East and North Africa as observed by the Tropospheric Emission Spectrometer instrument. Journal of Geophysical Research, 2009, 114, .	3.3	72
24	Why does surface ozone peak before a typhoon landing in southeast China?. Atmospheric Chemistry and Physics, 2015, 15, 13331-13338.	1.9	69
25	ENSO modulates wildfire activity in China. Nature Communications, 2021, 12, 1764.	5.8	69
26	The zonal structure of tropical O ₃ and CO as observed by the Tropospheric Emission Spectrometer in November 2004 – Part 1: Inverse modeling of CO emissions. Atmospheric Chemistry and Physics, 2009, 9, 3547-3562.	1.9	67
27	Assessment of foliage clumping effects on evapotranspiration estimates in forested ecosystems. Agricultural and Forest Meteorology, 2016, 216, 82-92.	1.9	64
28	Comparison of Bigâ€Leaf, Twoâ€Bigâ€Leaf, and Twoâ€Leaf Upscaling Schemes for Evapotranspiration Estimation Using Coupled Carbonâ€Water Modeling. Journal of Geophysical Research G: Biogeosciences, 2018, 123, 207-225.	1.3	64
29	Estimating crop biomass using leaf area index derived from Landsat 8 and Sentinel-2 data. ISPRS Journal of Photogrammetry and Remote Sensing, 2020, 168, 236-250.	4.9	64
30	Post-fire carbon dioxide fluxes in the western Canadian boreal forest: evidence from towers, aircraft and remote sensing. Agricultural and Forest Meteorology, 2003, 115, 91-107.	1.9	61
31	Continuous measurement of black carbon aerosol in urban Nanjing of Yangtze River Delta, China. Atmospheric Environment, 2014, 89, 415-424.	1.9	60
32	Observed vertical distribution of tropospheric ozone during the Asian summertime monsoon. Journal of Geophysical Research, 2009, 114, .	3.3	59
33	Quantifying the impact of model errors on top-down estimates of carbon monoxide emissions using satellite observations. Journal of Geophysical Research, 2011, 116, .	3.3	59
34	A global tropospheric ozone climatology from trajectory-mapped ozone soundings. Atmospheric Chemistry and Physics, 2013, 13, 10659-10675.	1.9	59
35	Diverse photosynthetic capacity of global ecosystems mapped by satellite chlorophyll fluorescence measurements. Remote Sensing of Environment, 2019, 232, 111344.	4.6	59
36	Comparison of boreal ecosystem model sensitivity to variability in climate and forest site parameters. Journal of Geophysical Research, 2001, 106, 33671-33687.	3.3	58

#	Article	IF	CITATIONS
37	An important mechanism of regional O ₃ transport for summer smog over the Yangtze River Delta in eastern China. Atmospheric Chemistry and Physics, 2018, 18, 16239-16251.	1.9	55
38	Drivers for the poor air quality conditions in North China Plain during the COVID-19 outbreak. Atmospheric Environment, 2021, 246, 118103.	1.9	54
39	Impacts of the East Asian monsoon on lower tropospheric ozone over coastal South China. Environmental Research Letters, 2013, 8, 044011.	2.2	52
40	A global ozone climatology from ozone soundings via trajectory mapping: a stratospheric perspective. Atmospheric Chemistry and Physics, 2013, 13, 11441-11464.	1.9	52
41	Observation and simulation of net primary productivity in Qilian Mountain, western China. Journal of Environmental Management, 2007, 85, 574-584.	3.8	51
42	Chinese Regulations Are Working—Why Is Surface Ozone Over Industrialized Areas Still High? Applying Lessons From Northeast US Air Quality Evolution. Geophysical Research Letters, 2021, 48, e2021GL092816.	1.5	50
43	Spatial scaling of net primary productivity using subpixel information. Remote Sensing of Environment, 2004, 93, 246-258.	4.6	48
44	Evaluation of Sentinel-2A Surface Reflectance Derived Using Sen2Cor in North America. IEEE Journal of Selected Topics in Applied Earth Observations and Remote Sensing, 2018, 11, 1997-2021.	2.3	48
45	Spatial distribution of carbon sources and sinks in Canada's forests. Tellus, Series B: Chemical and Physical Meteorology, 2022, 55, 622.	0.8	47
46	Measurement of lowâ€altitude CO over the Indian subcontinent by MOPITT. Journal of Geophysical Research, 2008, 113, .	3.3	47
47	Satellite mapping of CO emission from forest fires in Northwest America using MOPITT measurements. Remote Sensing of Environment, 2005, 95, 502-516.	4.6	45
48	Nitrogen Availability Dampens the Positive Impacts of CO ₂ Fertilization on Terrestrial Ecosystem Carbon and Water Cycles. Geophysical Research Letters, 2017, 44, 11,590.	1.5	45
49	The interactions between anthropogenic aerosols and the East Asian summer monsoon using RegCCMS. Journal of Geophysical Research D: Atmospheres, 2015, 120, 5602-5621.	1.2	44
50	Uplifting of carbon monoxide from biomass burning and anthropogenic sources to the free troposphere in East Asia. Atmospheric Chemistry and Physics, 2015, 15, 2843-2866.	1.9	44
51	Assessment of SMAP soil moisture for global simulation of gross primary production. Journal of Geophysical Research G: Biogeosciences, 2017, 122, 1549-1563.	1.3	44
52	Formation and Evolution Mechanisms for Two Extreme Haze Episodes in the Yangtze River Delta Region of China During Winter 2016. Journal of Geophysical Research D: Atmospheres, 2019, 124, 3607-3623.	1.2	43
53	Boreal ecosystems sequestered more carbon in warmer years. Geophysical Research Letters, 2006, 33, n/a-n/a.	1.5	42
54	Inter- and intra-annual variations of clumping index derived from the MODIS BRDF product. International Journal of Applied Farth Observation and Geoinformation, 2016, 44, 53-60	1.4	42

#	Article	IF	CITATIONS
55	Improved assessment of gross and net primary productivity of Canada's landmass. Journal of Geophysical Research G: Biogeosciences, 2013, 118, 1546-1560.	1.3	41
56	Characteristics of ozone and particles in the near-surface atmosphere in the urban area of the Yangtze River Delta, China. Atmospheric Chemistry and Physics, 2019, 19, 4153-4175.	1.9	41
57	Spatial and temporal variation of MOPITT CO in Africa and South America: A comparison with SHADOZ ozone and MODIS aerosol. Journal of Geophysical Research, 2004, 109, .	3.3	40
58	Collective impacts of biomass burning and synoptic weather on surface PM2.5 and CO in Northeast China. Atmospheric Environment, 2019, 213, 64-80.	1.9	39
59	Application of SCIAMACHY and MOPITT CO total column measurements to evaluate model results over biomass burning regions and Eastern China. Atmospheric Chemistry and Physics, 2011, 11, 6083-6114.	1.9	37
60	Rising surface ozone in China from 2013 to 2017: A response to the recent atmospheric warming or pollutant controls?. Atmospheric Environment, 2021, 246, 118130.	1.9	36
61	Spatial distribution of net primary productivity and evapotranspiration in Changbaishan Natural Reserve, China, using Landsat ETM+ data. Canadian Journal of Remote Sensing, 2004, 30, 731-742.	1.1	35
62	Highâ€resolution tropospheric ozone fields for INTEX and ARCTAS from IONS ozonesondes. Journal of Geophysical Research, 2010, 115, .	3.3	35
63	The surface aerosol optical properties in the urban area of Nanjing, west Yangtze River Delta, China. Atmospheric Chemistry and Physics, 2017, 17, 1143-1160.	1.9	34
64	Quantifying stratosphere-troposphere transport of ozone using balloon-borne ozonesondes, radar windprofilers and trajectory models. Atmospheric Environment, 2019, 198, 496-509.	1.9	34
65	Characterizing regional aerosol pollution in central China based on 19 years of MODIS data: Spatiotemporal variation and aerosol type discrimination. Environmental Pollution, 2020, 263, 114556.	3.7	34
66	Climatic analysis of satellite aerosol data on variations of submicron aerosols over East China. Atmospheric Environment, 2015, 123, 392-398.	1.9	31
67	Large horizontal gradients in atmospheric CO at the synoptic scale as seen by spaceborne Measurements of Pollution in the Troposphere. Journal of Geophysical Research, 2006, 111, .	3.3	29
68	Influence of interannual variations in transport on summertime abundances of ozone over the Middle East. Journal of Geophysical Research, 2011, 116, .	3.3	29
69	Optimization of water uptake and photosynthetic parameters in an ecosystem model using tower flux data. Ecological Modelling, 2014, 294, 94-104.	1.2	29
70	Absorption coefficient of urban aerosol in Nanjing, west Yangtze River Delta, China. Atmospheric Chemistry and Physics, 2015, 15, 13633-13646.	1.9	29
71	The direct effects of black carbon aerosols from different source sectors in East Asia in summer. Climate Dynamics, 2019, 53, 5293-5310.	1.7	29
72	Systematic classification of circulation patterns and integrated analysis of their effects on different ozone pollution levels in the Yangtze River Delta Region, China. Atmospheric Environment, 2020, 242, 117760.	1.9	28

#	Article	IF	CITATIONS
73	Title is missing!. Mitigation and Adaptation Strategies for Global Change, 2000, 5, 143-169.	1.0	26
74	Satellite-Observed Variations and Trends in Carbon Monoxide over Asia and Their Sensitivities to Biomass Burning. Remote Sensing, 2020, 12, 830.	1.8	26
75	Continuous rise of the tropopause in the Northern Hemisphere over 1980–2020. Science Advances, 2021, 7, eabi8065.	4.7	26
76	Atmospheric transport drives regional interactions of ozone pollution in China. Science of the Total Environment, 2022, 830, 154634.	3.9	26
77	Characteristics of intercontinental transport of tropospheric ozone from Africa to Asia. Atmospheric Chemistry and Physics, 2018, 18, 4251-4276.	1.9	24
78	Surface Ozone in the Yangtze River Delta, China: A Synthesis of Basic Features, Meteorological Driving Factors, and Health Impacts. Journal of Geophysical Research D: Atmospheres, 2021, 126, e2020JD033600.	1.2	24
79	Ozone variability induced by synoptic weather patterns in warm seasons of 2014–2018 over the Yangtze River Delta region, China. Atmospheric Chemistry and Physics, 2021, 21, 5847-5864.	1.9	24
80	On the CO2 exchange between the atmosphere and the biosphere: the role of synoptic and mesoscale processes. Tellus, Series B: Chemical and Physical Meteorology, 2004, 56, 194-212.	0.8	24
81	Interaction between the Black Carbon Aerosol Warming Effect and East Asian Monsoon Using RegCM4. Journal of Climate, 2018, 31, 9367-9388.	1.2	23
82	Regional CO ₂ fluxes from 2010 to 2015 inferred from GOSAT XCO ₂ retrievals using a new version of the Global Carbon Assimilation System. Atmospheric Chemistry and Physics, 2021, 21, 1963-1985.	1.9	23
83	The optical properties, physical properties and direct radiative forcing of urban columnar aerosols in the Yangtze River Delta, China. Atmospheric Chemistry and Physics, 2018, 18, 1419-1436.	1.9	22
84	Impacts of Synoptic Weather Patterns and their Persistency on Free Tropospheric Carbon Monoxide Concentrations and Outflow in Eastern China. Journal of Geophysical Research D: Atmospheres, 2018, 123, 7024-7046.	1.2	22
85	Exploring SMAP and OCO-2 observations to monitor soil moisture control on photosynthetic activity of global drylands and croplands. Remote Sensing of Environment, 2019, 232, 111314.	4.6	21
86	Ozone affected by a succession of four landfall typhoons in the Yangtze River Delta, China: major processes and health impacts. Atmospheric Chemistry and Physics, 2020, 20, 13781-13799.	1.9	21
87	Regional transport patterns for heavy PM2.5 pollution driven by strong cold airflows in Twain-Hu Basin, Central China. Atmospheric Environment, 2022, 269, 118847.	1.9	20
88	Importance of Bias Correction in Data Assimilation of Multiple Observations Over Eastern China Using WRFâ€Chem/DART. Journal of Geophysical Research D: Atmospheres, 2020, 125, e2019JD031465.	1.2	18
89	Fine-scale leaf chlorophyll distribution across a deciduous forest through two-step model inversion from Sentinel-2 data. Remote Sensing of Environment, 2021, 264, 112618.	4.6	18
90	A Vertical Diffusion Scheme to estimate the atmospheric rectifier effect. Journal of Geophysical Research, 2004, 109, n/a-n/a.	3.3	17

#	Article	IF	CITATIONS
91	Carbon monoxide climatology derived from the trajectory mapping of global MOZAIC-IAGOS data. Atmospheric Chemistry and Physics, 2016, 16, 10263-10282.	1.9	16
92	Foreign influences on tropospheric ozone over East Asia through global atmospheric transport. Atmospheric Chemistry and Physics, 2019, 19, 12495-12514.	1.9	16
93	Carbon monoxide (CO) maximum over the Zagros mountains in the Middle East: Signature of mountain venting?. Geophysical Research Letters, 2006, 33, .	1.5	15
94	Correction to "Analysis of the summertime buildup of tropospheric ozone abundances over the Middle East and North Africa as observed by the Tropospheric Emission Spectrometer Instrument― Journal of Geophysical Research, 2009, 114, .	3.3	15
95	Regional and hemispheric influences on temporal variability in baseline carbon monoxide and ozone over the Northeast US. Atmospheric Environment, 2017, 164, 309-324.	1.9	15
96	Simulations of seasonal and inter-annual variability of gross primary productivity at Takayama with BEPS ecosystem model. Agricultural and Forest Meteorology, 2005, 134, 143-150.	1.9	14
97	Impacts of atmospheric transport and biomass burning on the inter-annual variation in black carbon aerosols over the Tibetan Plateau. Atmospheric Chemistry and Physics, 2020, 20, 13591-13610.	1.9	14
98	Impacts of anthropogenic and natural sources on free tropospheric ozone over the Middle East. Atmospheric Chemistry and Physics, 2016, 16, 6537-6546.	1.9	12
99	The Impacts of Meteorology on the Seasonal and Interannual Variabilities of Ozone Transport From North America to East Asia. Journal of Geophysical Research D: Atmospheres, 2017, 122, 10,612.	1.2	12
100	Meteorological Influences on Seasonal Variation of Fine Particulate Matter in Cities over Southern Ontario, Canada. Advances in Meteorology, 2014, 2014, 1-15.	0.6	11
101	Crop Biomass Mapping Based on Ecosystem Modeling at Regional Scale Using High Resolution Sentinel-2 Data. Remote Sensing, 2021, 13, 806.	1.8	11
102	Exploring the ozone pollution over the western Sichuan Basin, Southwest China: The impact of diurnal change in mountain-plains solenoid. Science of the Total Environment, 2022, 839, 156264.	3.9	11
103	Stratospheric ozone loss in the Arctic winters between 2005 and 2013 derived with ACE-FTS measurements. Atmospheric Chemistry and Physics, 2019, 19, 577-601.	1.9	10
104	Tree-ring recorded variations of 10 heavy metal elements over the past 168 years in southeastern China. Elementa, 2021, 9, .	1.1	10
105	The Role of Natural Halogens in Global Tropospheric Ozone Chemistry and Budget Under Different 21st Century Climate Scenarios. Journal of Geophysical Research D: Atmospheres, 2021, 126, e2021JD034859.	1.2	10
106	Nocturnal surface radiation cooling modulated by cloud cover change reinforces PM2.5 accumulation: Observational study of heavy air pollution in the Sichuan Basin, Southwest China. Science of the Total Environment, 2021, 794, 148624.	3.9	9
107	Regional Climate Responses in East Asia to the Black Carbon Aerosol Direct Effects from India and China in Summer. Journal of Climate, 2020, 33, 9783-9800.	1.2	9
108	Long Temporal Analysis of 3-km MODIS Aerosol Product Over East China. IEEE Journal of Selected Topics in Applied Earth Observations and Remote Sensing, 2017, 10, 2478-2490.	2.3	8

#	Article	IF	CITATIONS
109	Estimating wildfire-generated ozone over North America using ozonesonde profiles and a differential back trajectory technique. Atmospheric Environment: X, 2020, 7, 100078.	0.8	8
110	Positive and negative influences of typhoons on tropospheric ozone over southern China. Atmospheric Chemistry and Physics, 2021, 21, 16911-16923.	1.9	8
111	Sensitivity of climate effects of black carbon in China to its size distributions. Atmospheric Research, 2017, 185, 118-130.	1.8	7
112	Seasonal variations in energy exchange and evapotranspiration of an oasisâ€desert ecotone in an arid region. Hydrological Processes, 2021, 35, e14364.	1.1	7
113	Effects of Improved Simulation of Precipitation on Evapotranspiration and Its Partitioning Over Land. Geophysical Research Letters, 2022, 49, .	1.5	7
114	Importance of Shaded Leaf Contribution to the Total GPP of Canadian Terrestrial Ecosystems: Evaluation of MODIS GPP. Journal of Geophysical Research G: Biogeosciences, 2020, 125, e2020JG005917.	1.3	6
115	Impact of regional transport on high ozone episodes in southeast coastal regions of China. Atmospheric Pollution Research, 2022, 13, 101497.	1.8	5
116	Transport of substantial stratospheric ozone to the surface by a dying typhoon and shallow convection. Atmospheric Chemistry and Physics, 2022, 22, 8221-8240.	1.9	4
117	A teleconnection between sea surface temperature in the central and eastern Pacific and wintertime haze variations in southern China. Theoretical and Applied Climatology, 2021, 143, 349-359.	1.3	3
118	Quantifying spatio-temporal variations of evapotranspiration over a heterogeneous terrain in the Arid regions of Northwestern China International Journal of Remote Sensing, 2021, 42, 3231-3254.	1.3	3
119	Characterizing pollution weather patterns using satellite carbon monoxide data. , 2016, , .		2
120	Biases of Global Tropopause Altitude Products in Reanalyses and Implications for Estimates of Tropospheric Column Ozone. Atmosphere, 2021, 12, 417.	1.0	2
121	Special Issue "Remote Sensing of Greenhouse Gases and Air Pollution― Remote Sensing, 2021, 13, 2057.	1.8	2
122	Regional Forecasting of Fine Particulate Matter Concentrations: A Novel Hybrid Model Based on Principal Component Regression and EOF. Earth and Space Science, 2021, 8, e2021EA001694.	1.1	2
123	Vertical sensitivity of satellite remote sensing of atmospheric carbon monoxide. , 2015, , .		1
124	Net primary productivity distribution in China from a process model driven by remote sensing. , 0, , .		0
125	National Scale Forest Information Extraction from Coarse Resolution Satellite Data, Part 2. , 2003, , 359-387.		0
126	Temporal and spatial variations in ozone over Asian free troposphere. , 2017, , .		0

	JA	ne Liu	
#	Article	IF	CITATIONS
127	Editorial: The Evolution of the Stratospheric Ozone. Frontiers in Earth Science, 2021, 9, .	0.8	ο